Soil Dynamics and Earthquake Engineering 92 (2017) 388–396

Contents lists available at ScienceDirect

Soil Dynamics and Earthquake Engineering

journal homepage: www.elsevier.com/locate/soildyn

Liquefaction characteristics of gravelly soil under cyclic loading with constant strain amplitude by experimental and numerical investigations

Yong Wang[a,b,*], Yan-Li Wang[c]

[a] State Key Laboratory of Geomechanics and Geotechnical Engineering, Institute of Rock and Soil Mechanics, Chinese Academy of Sciences, Wuhan 430071, China

[b] State Key Laboratory of Geomechanics and Deep Underground Engineering, China University of Mining and Technology, Xuzhou 221116, China

[c] Key Laboratory of Geotechnical Mechanics and Engineering of the Ministry of Water Resources, Yangtze River Scientific Research Institute, Wuhan 430010, China

ARTICLE INFO

Keywords:
Gravel soil
Liquefaction
Gravel content
DEM
CT scan
Force-chain
Meso-mechanism

ABSTRACT

In order to investigate the liquefaction behavior and meso-mechanism of gravelly soil under cyclic loading with constant strain amplitude, the undrained dynamic triaxial test, CT scan test and numerical simulations by discrete element method (DEM) are performed. Effects of gravel content and the evolution of liquefaction nmeso-mechanism are analyzed respectively. Test Results show that the liquefaction resistance of gravelly soil increases considerably with the increasing gravel content due to growing in number of gravel-to-gravel contact. DEM simulations reflect the macro mechanical property of saturated gravelly soil in the cyclic triaxial test, and show anisotropy is the most important mechanical properties of gravelly soil liquefaction under cyclic loading with constant strain amplitude. In process of the liquefaction, the backbone force-chain is gradually destroyed, and magnitude of normal contact force decreases to zero until initial liquefaction. Both of the fabric and force-chain evolution demonstrate a consistent deflection of the principal stress axis.

1. Introduction

Gravelly soil is often mistaken as non-liquefiable because of its coarser particles, and good permeability. As the natural foundation or earthwork filling materials, it is widely used in constructions of the dam filling, marine reclamation land, and highway and high-speed railway roadbed due to good qualities such as high strength, low compressibility, low cost and so on. However, the phenomenon of gravel soil liquefaction had been observed in worldwide earthquakes during the last 50 years [1–9]. In fact, a few of laboratory tests also proved the possibility of its liquefaction. Wong et al. [10], Baneriee et al. [11] performed a series of undrained cyclic triaxial tests, and found that gravel soil has "initial liquefaction" phenomenon as same as sand. Liu et al. [12], Wang et al. [13] performed comparison of the shaking table test and undrained cyclic triaxial test of gravel soil liquefaction. And test results showed the liquefaction properties were mainly determined by coefficient of permeability and drainage conditions, and related to the relative density and volume compressibility. Evans et al. [14] carried out a series of undrained cyclic triaxial tests on gravelly soils with gravel contents of 0%, 20%, 40%, 60%, and 100%. And results showed the liquefaction resistance of sand-gravel composites increased significantly with the increasing gravel content. Hatanaka [15] performed a series of large dynamic triaxial tests of nature and remolded specimens of gravel soil, and study the effects of sample disturbance on the liquefaction strength. By the cyclic triaxial tests on reconstituted gravel soil specimens, Kokusho et al. [16] concluded that the undrained cyclic strength of such soils mainly depended on the relative density rather than particle gradation. Chang et al. [17] performed a series of undrained dynamic simple shear tests to study the liquefaction characteristics of gap-graded gravelly soils with no fines content in K_0 condition. And the test results revealed that a linear relationship existed between shear wave velocity and sand content for the gravel-like sandy gravels at a given gravel skeleton void ratio, and also existed between shear wave velocity and the gravel content for sand-like gravelly sand at a given sand skeleton void ratio.

In the last decade, some studies on the liquefaction discrimination method have been carried out for gravelly soil. Lin et al. [18] performed Instrumented Large Hammer Penetration Test (LHPT) and shear wave velocity (Vs) measurements in a liquefied gravelly deposit site during the Chi-Chi earthquake to evaluate the liquefaction resistance. Cao et al. [19] developed a probabilistic dynamic penetration test for predicting liquefaction resistance of gravelly soils based on the field

* Corresponding author at: State Key Laboratory of Geomechanics and Geotechnical Engineering, Institute of Rock and Soil Mechanics, Chinese Academy of Sciences, Wuhan 430071, China.

E-mail address: wang831yong@126.com (Y. Wang).

http://dx.doi.org/10.1016/j.soildyn.2016.10.029
Received 12 February 2015; Received in revised form 10 March 2016; Accepted 23 October 2016
0267-7261/ © 2016 Elsevier Ltd. All rights reserved.

test during 2008 Wenchuan earthquake of China. It should be noted that most of the studies focused on the liquefaction resistance strength, development features of pore pressure and liquefaction evaluation, but few concerned the meso-mechanism of gravelly soil liquefaction. Typical gravelly soil is composed of a large number of solid particles, due to the inhomogeneity of particle shape, size, location, and random distribution, so it is a multi-scale structure necessarily, including the macrostructure, mesostructure, and microstructure. Generally, the macrostructure element size of soil mass is between 2 mm-10 m; the size of mesostructure is between 0.05–2 mm; and the size of microstructure is usually less than 0.05mm [20]. In this paper, the liquefaction property and meso-mechanism of gravelly soil under cyclic loading with constant strain amplitude are emphatically investigated. A series of undrained dynamic triaxial tests on saturated gravelly soil with different gravel content under the constant-amplitude strain cycle mode were performed with the GDS dynamic triaxial system. Before the tests, the initiating structure of the samples with different gravel content was scanned by computed tomography technology (CT). Then numerical simulations on the tests of saturated gravelly soil liquefaction were conducted by the Particle Flow Code(PFC). Through comparative analysis, a number of features of liquefaction behavior and the evolution law of meso-mechanism on gravel soil were studied.

2. Experimental procedures and results

2.1. Sample preparation

Gravelly soils sampled from the Hub Dam (Site II) of Shitou Gorge in Menyuan County, Qinghai Province of China with grain sizes not exceeding 20 mm were used. Next, the dried soil samples were screened with 20 mm, 10 mm, 5 mm, 2 mm, and 1 mm screens successively. The size of particles between 2 mm and 20 mm were selected as gravel, whereas those particles less than 2 mm were selected as sand and fine.

Undrained dynamic triaxial tests were carried out to examine the effect of gravel content on the liquefaction characteristics of saturated gravelly soil under cyclic loading with constant strain amplitude. In the test, cylindrical specimens 101 mm diameter and 200 mm high were used. In preparing the specimen, sand and gravel components of the soil were mixed that the gravel contents by weight P_2 were 50%,60%,70%,80%. Grain size distributions are shown in Fig. 1 and grain size parameters are listed in Table 1.

To determine the relative density of the gravelly soil, maximum and minimum dry densities were obtained from 50–80% of gravel contents. The maximum density was determined by the surface vibratory compaction method. The minimum density was determined by the fixed volume method. Fig. 2 shows the relationship between the maximum and minimum dry densities versus gravel content for the materials tested. The maximum dry density increases significantly with increasing gravel content from 50–60%, when gravel content beyond 60% the trend was reversed, and the maximum dry density decreases with increasing gravel content. While the minimum dry density decreases monotonously with increasing gravel content from 50–80%.

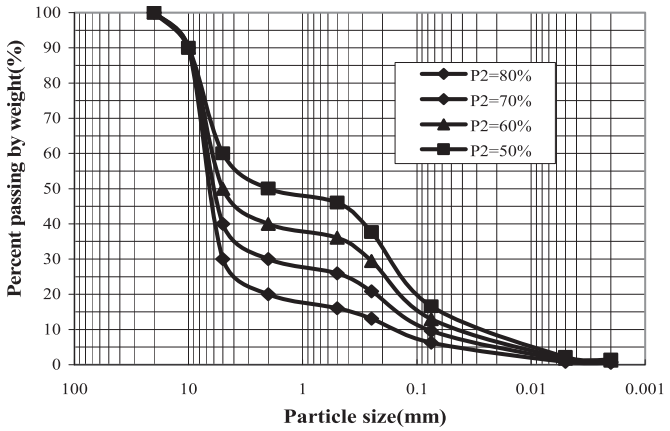

Fig. 1. Grain size distribution curve of test soil.

Table 1
Grain size parameters of test soil.

Gravel content P_2 (%)	d_{10} mm	d_{50} mm	d_{70} mm	d_{60} mm	d_{30} mm	C_u	C_c
80	0.139	6.524	7.863	7.170	5.000	51.505	25.044
70	0.078	5.988	7.579	6.779	2.000	86.925	7.567
60	0.068	5.000	7.170	6.183	0.262	91.580	0.164
50	0.066	2.000	6.503	5.000	0.156	75.742	0.074

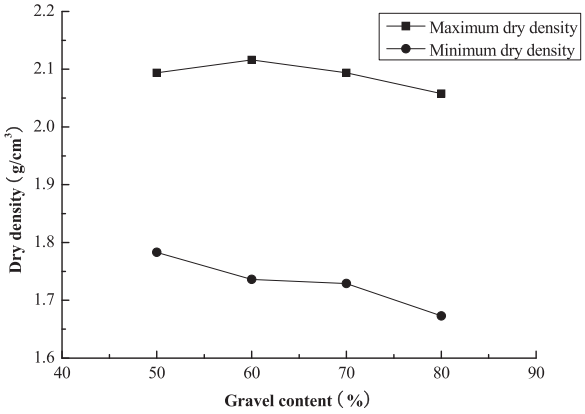

Fig. 2. Maximum and minimum densities versus gravel content.

Specimens are prepared to a constant relative density equal to 55%. The remolded samples are prepared by using multi-level wet pounding method, and the samples are composed of three layers. According to dry density and the design of each layer of soil moisture content of the soil samples, the weight of each layer is determined and the soil of each layer is compacted to corresponding height. The interface between the two layers is scarified to ensure the upper and lower layers are in good contacts.

2.2. CT scan tests

In order to study the microstructure of the gravelly soil with different gravel content, the computed tomography (CT) was applied to obtain CT images at different depth of the gravelly soil specimens for a constant value of relative density. Scanning position diagram is shown in Fig. 3. Three scanning layers were set in every specimen. CT scanning images at different depth of the gravelly soil with different gravel content are shown in Fig. 4. For gravel contents between 50% and 80%, it appears that sand particles float in the gravel matrix, gravel-to-gravel contact is separated by the sand and fines at lower

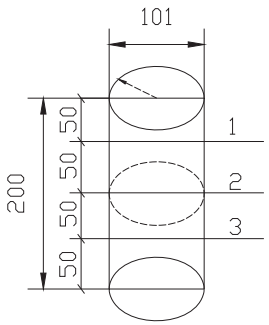

Fig. 3. Scanning position diagram (Unit: mm).

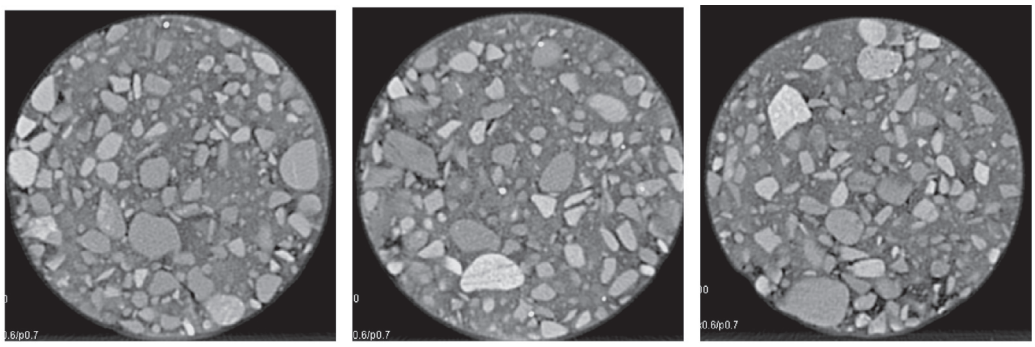

(a) Specimen with 50% gravel

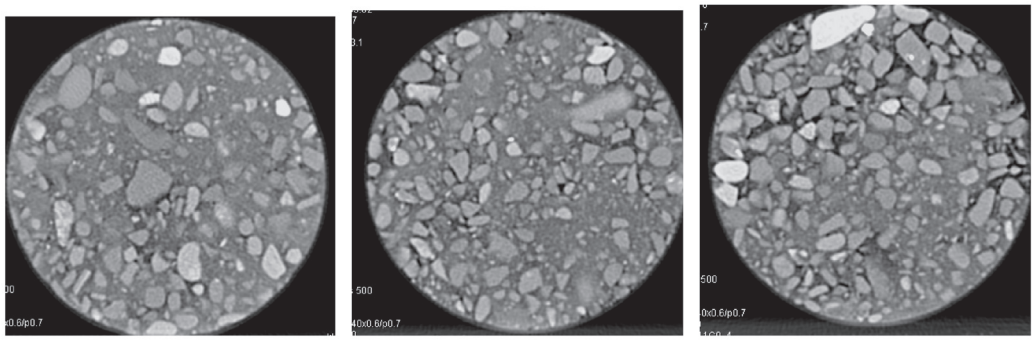

(b) Specimen with 60% gravel

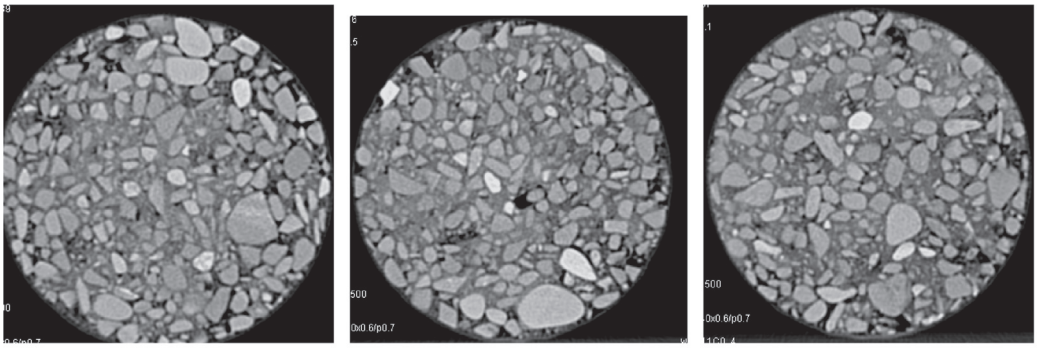

(c) Specimen with 70% gravel

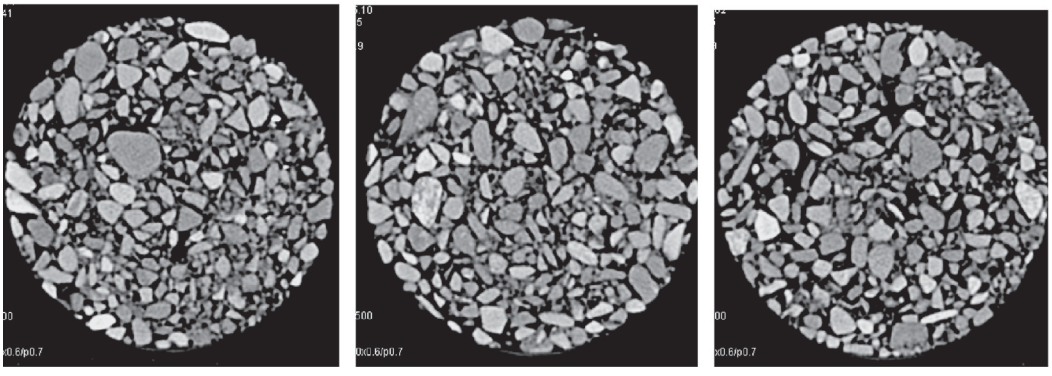

(d) Specimen with 80% gravel

Fig. 4. CT scanning images of gravelly soil specimens at different depth.

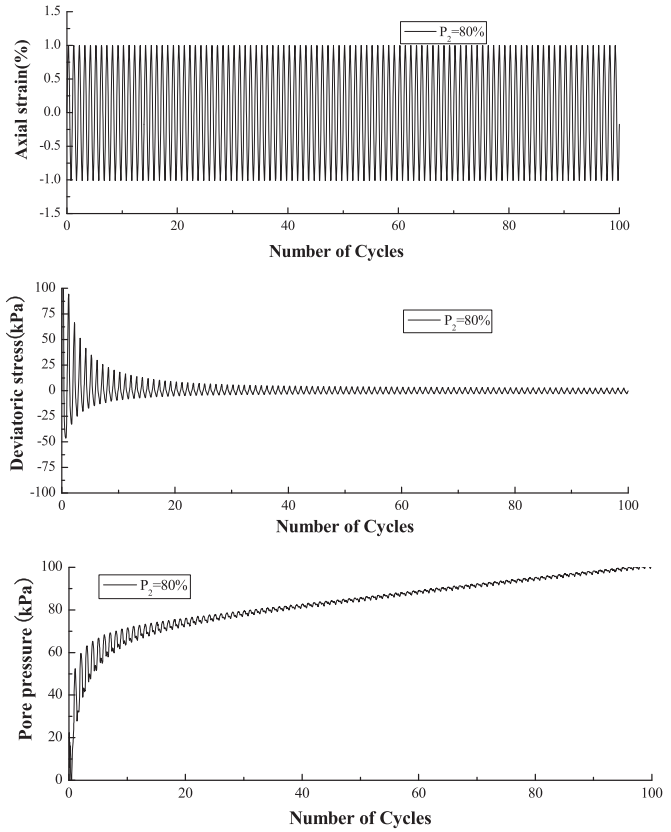

Fig. 5. Dynamic triaxial test curve of liquefaction behavior on typical saturated gravelly soil with constant strain amplitude.

gravel content. With increasing gravel content, the sand and fines does not completely fill the gravel voids and gravel-to-gravel contact increases.

2.3. Undrained dynamic triaxial tests with constant strain amplitude

After CT Scanning, the specimen was fully saturated by hydraulic saturation method and back pressure saturation method. The specimens were percolated with de-aired water from the bottom of the specimen towards the top while the specimens were subjected to about 20–30kPa effective confining pressure. Then the cell and pore water pressure were slowly increased simultaneously to achieve a B value that was typically greater than 0.95. The specimens were isotropically consolidated under an effective confining stress equal to 100 kPa. The standard of isotropic consolidation can be deemed to be reached when the volumetric change of the specimen keep invariable in 5 min. In the undrained cyclic loading tests, the axial strain was cyclically controlled by sinusoidal waves with the frequency of 1 Hz and the strain amplitude is 1%. The cyclic loading was continued until initial liquefaction occurred until the pore water pressure became equal to the confining pressure. The pore water pressure, axial strain and axial stress were recorded during the cyclic loading.

Dynamic triaxial test curve of liquefaction behavior on typical saturated gravelly soil with constant strain amplitude is shown in Fig. 5. Cyclic axial strain, cyclic axial stress and generated pore pressure during undrained cyclic testing at a predetermined confining pressure following consolidation can be measured utilizing the GDS dynamic triaxial apparatus.

Fig. 5 shows clearly that the axial strain amplitude holds constant regularly and consistently in the dynamic triaxial test. Deviatoric stress amplitude decays slowly in the early stages of testing with constant strain amplitude. As vibration continues, the deviatoric stress amplitude decays much more rapidly. When the dynamic pore pressure was

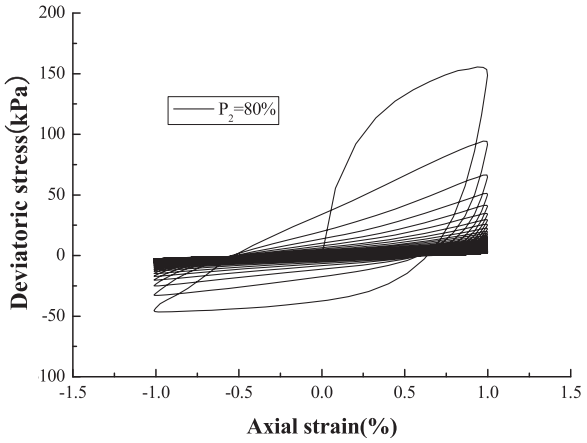

Fig. 6. Stress-strain response of typical saturated gravelly soil with constant strain amplitude.

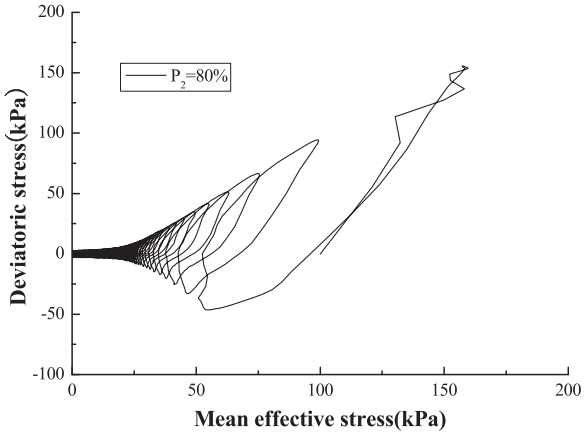

Fig. 7. Effective stress path curve of typical saturated gravelly soil with constant strain amplitude.

accumulated to the initial effective consolidation pressure, liquefaction occurred, and deviatoric stress amplitude decays catastrophically. The pore pressure took on a fluctuant increasing process in the dynamic triaxial test with constant strain amplitude. As the vibration continues, the structure of the soil specimen changes, and soil particles tend to be more closely due to sliding. Pore water pressure accumulates quickly, and deviatoric stress amplitude decays rapidly. At this time, most of load on the soil samples is born by the pore water. When liquefaction occurred, the bearing capacity reduced to zero.

Stress-strain response and effective stress path curve of typical saturated gravelly soil with constant strain amplitude are shown in Figs. 6 and 7 respectively. The stress-strain curve changes from sloping to horizontal direction due to the deviatoric stress amplitude attenuation. At this time, due to the constant rise of the pore water pressure, the effective stress acting on the soil skeleton reduced sharply, the strength of soil loss greatly, the effective stress path moves to the origin until the initial liquefaction occurred.

Fig. 8 is a plot of number of strain cycles required for initial liquefaction of gravelly soil at 55% relative density with gravel contents of 50%, 60%, 70%, and 80%. It can be seen that the more gravel content, the more strain cycles required to initial liquefaction, which shows that the liquefaction resistance of the gravelly soil specimens increases significantly with the gravel content. Those can be explained from the microstructure of gravelly soil obtained by CT scan test.

The gravelly soil is assumed to be composed of coarse grains and fine grains, the size of which is distinguished by 2 mm. The microstructure characteristics of gravelly soil can be divided into two types according to relevant different roles of coarse and fine grains. In type

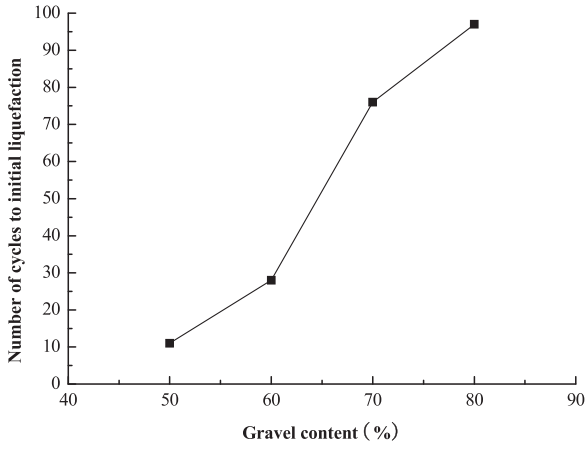

Fig. 8. Effect of gravel content on the strain cycles required for initial liquefaction of gravelly soil.

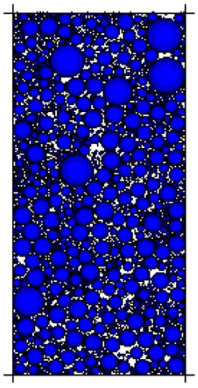

Fig. 9. The numerical model of specimen.

(1), the gravelly soil skeleton is formed by contact between fine grains (sand particles), and the mechanical behavior is affected primarily by the fine grain contacts. In type (2), the gravelly soil skeleton is formed by contact between coarser grains (gravel particles), and the mechanical behavior is affected primarily by the coarser grain contacts. When sand particles mixed into gravel particles forming the gravelly soil, because sand content is less, and the gravel content is more, coarse grains form skeleton voids by mutual arrangement, while the fine grains do not occupy the voids between the coarse grains but dissociate in the skeleton voids in a great measure. Liquefaction resistance of gravelly soil is manly determined by the coarse grains. The meso-structure of the tested soil in this study belongs to the type (2), and it can be verified by the CT scan test results shown in Fig. 4. With increasing gravel content, the skeleton voids between the coarse grains become smaller, which makes the gravel-to-gravel contact increase, and the liquefaction resistance of gravelly soil also increases with it.

3. DEM simulation of the dynamic triaxial test of typical gravelly soil

The discrete element method (DEM) software, two-dimensional particle flow code, PFC^{2D} (Itasca Consulting Group, Inc., Minnesota), is used here. Features of the numerical specimens and details of the simulation procedures in the biaxial tests including the sample generation are given in Wang [21]. Essential points are summarized as follows to facilitate the discussion.

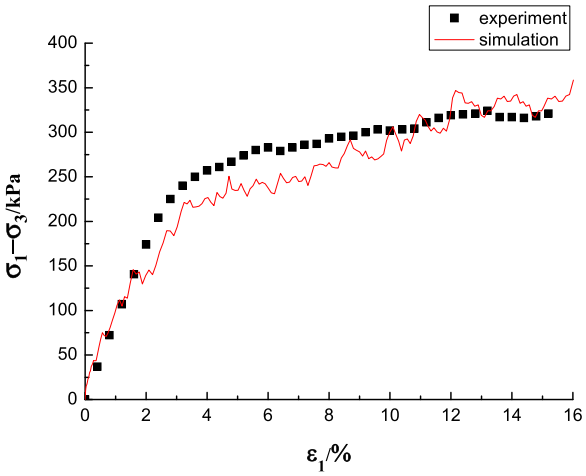

Fig. 10. Comparison of stress-stain curves between the numerical simulation and the experiment.

3.1. Numerical Specimen

With reference to the physical specimen prepared for the triaxial tests, the numerical specimen is 200 mm wide and 400 mm high, as illustrated in Fig. 9, was made by a series of particles. The gravelly soil with gravel content 80% is selected as the simulation object. Considering that the gravelly soil samples contain different particle sizes (ranging from 0 mm to 20 mm), a subprogram for discrete element simulation analysis of different particle grading soil samples is used to simulate the real particle grading. It is well known that mesoscopic parameters have an important effect on macroscopic mechanical properties in DEM simulations. For mesoscopic simulation of gravelly soil using PFC^{2D}, the determination of mesoscopic physics mechanics parameters is more troublesome but necessary. Due to the complication and difficulty of the simulation of gravelly soil liquefaction in the cyclic triaxial test, the mesoscopic parameters are determined by the results of conventional undrained triaxial compression test of the same gravelly soil. The associated input parameters are summarized in Table 2. The comparison of stress-stain curves of the numerical simulation and the experiment is shown in Fig. 10.

3.2. Biaxial tests simulation

The simulation of biaxial tests follows the standard procedure of the dynamic triaxial tests, which is also divided into two stages: consolidation and undrained cyclic loading with constant strain amplitude. Numerical method that indirectly considers fluid effects is known as constant volume method. A constant volume method is based on the almost constant volume of saturated soil specimens under undrained loading.

The consolidation was carried out by applying loading onto the top plate and bottom plate. The confining pressure was constantly checked to maintain the target value throughout the test. The shearing stage was strain-controlled and carried out by moving the top and bottom plate at a constant velocity of 0.1 m/s in the opposite direction, meanwhile moving the left and right plate at a constant velocity of

Table 2
Parameters of particles used in DEM simulations.

Sample size (mm)	Particle proportion (kg/m^3)	Porosity	Friction coefficient	Normal contact stiffness (N/m)	Shear contact stiffness (N/m)	Confining pressure (kPa)
200×400	2752	0.322	0.6	8e7	8e7	100

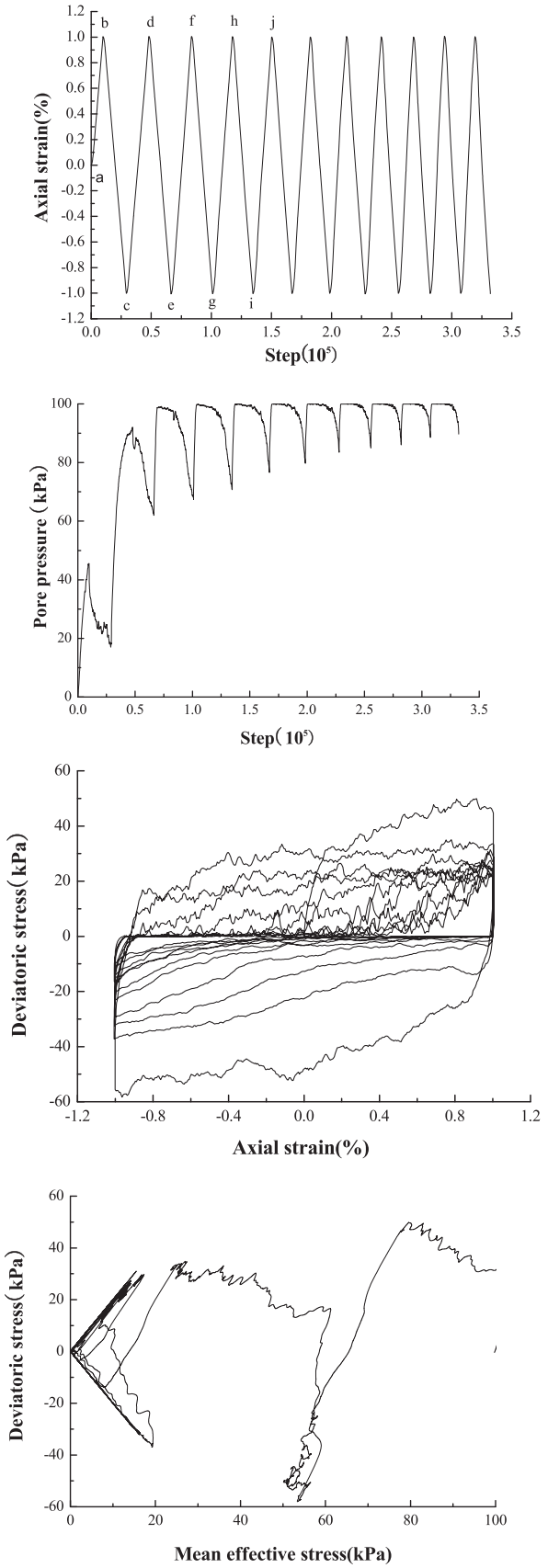

Fig. 11. Numerical biaxial test results of saturated gravelly soil under cyclic loading with constant strain amplitude.

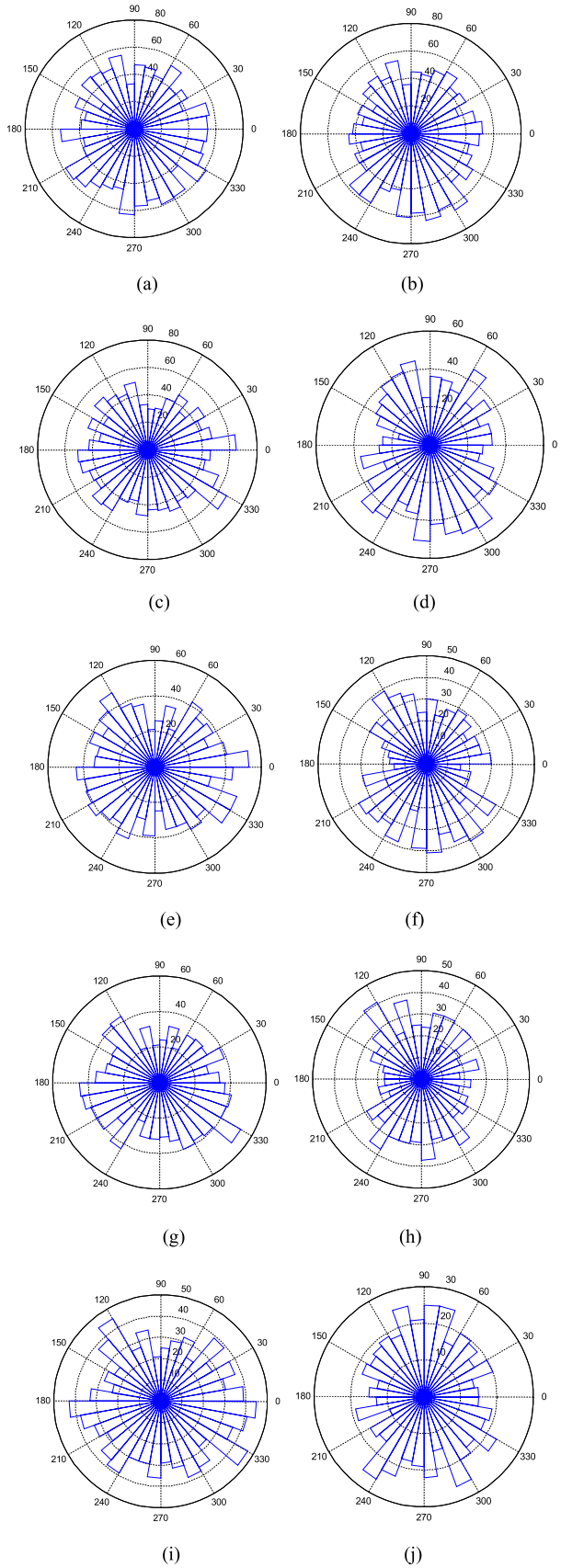

Fig. 12. Contact normal evolution of saturated gravelly soil specimen under cyclic loading with constant strain amplitude.

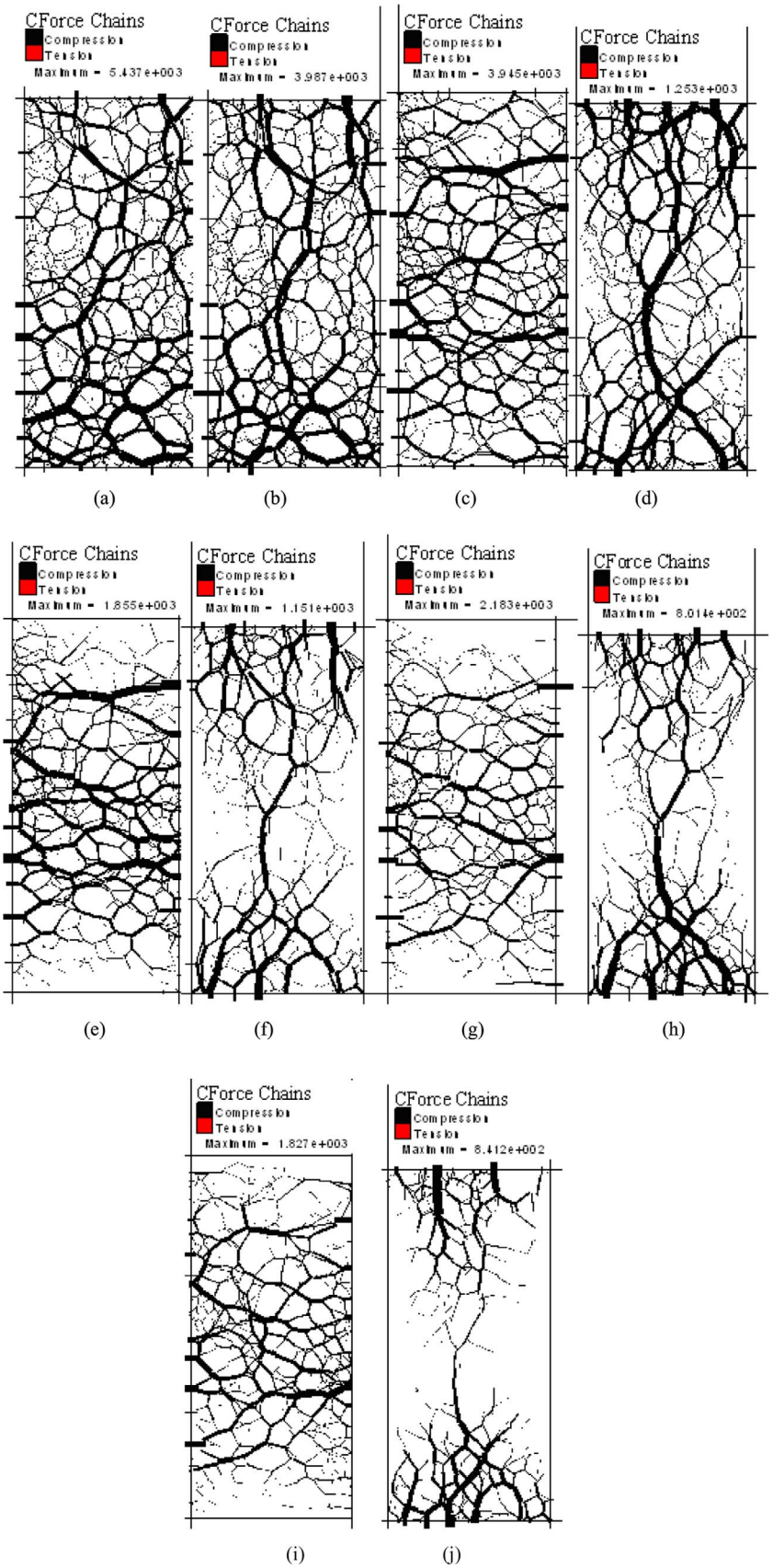

Fig. 13. Force-chain evolution of saturated gravelly soil specimen under cyclic loading with constant strain amplitude (the thickness of each line represents the magnitude of the contact force).

0.05 m/s in the opposite direction to maintain the same volume of the sample. The axial strain, stress–strain, effective stress path, and dynamic pore pressure responses were monitored during the biaxial test.

3.3. Numerical simulations results

3.3.1. General macro-mechanical features

Fig. 11 shows the numerical biaxial test results of the typical saturated gravelly soil under cyclic loading with constant strain amplitude, including the time-history curves of dynamic strain and dynamic pore pressure, stress-strain curve and effective stress path. The numerical simulation results can clearly reflect the liquefaction characteristics of the saturated gravelly soil under cyclic loading with constant strain amplitude. With increasing vibration cycles, the pore pressure is cumulative until the "initial liquefaction" occurred and stress-strain hysteresis curve gradually leans in the horizontal with a recession in stiffness of the specimen. The accumulation of dynamic pore pressure causes the mean effective principal stress of specimens to decrease and the effective stress path moves toward the original point.

From the above analysis, the numerical simulation results can well reflect the general rule of liquefaction characteristics of the saturated gravelly soil in dynamic triaxial tests, but also there are some differences between them. Numerical simulation in the two-dimensional plane space using pure disc particles in sample, but gravelly soil is composed of a large number of solid particles with the inhomogeneity of different particle shape, size, and random distribution. The fabric distribution also has a three-dimensional effect, so the numerical simulation in the two-dimensional is only qualitative description of liquefaction characteristics of gravelly soil. Compared with the laboratory test results, the gravelly soil is more prone to liquefaction in the numerical simulation without regard to space effect. In addition, the area of porosity in two-dimensional numerical simulation is different from the volume of a porosity, which can result in the quantitative discrepancies between the results of them.

3.3.2. Fabric and force-chain evolution

Fabric appears to have an important role controlling the behavior of granular material, which has been recognized. Fabric is usually defined as the spatial arrangement of particles [22]. The distribution of the contact normal is an important part of the fabric, which is a common indicator reflecting material anisotropy. Fig. 12 shows the fabric evolution of saturated gravelly soil specimen at a, b, c, d, e, f, g, h, i and j in Fig. 11 of the cyclic loading process with constant strain amplitude. The anisotropy evolution of the saturated gravelly soil specimen before and after the liquefaction can be observed clearly. It can be seen from Fig. 12 that the contact normal are nearly isotropic at the initial stage, and become anisotropic immediately when cyclic stain starts. The contact normal angle has strong peaks at 90°and 270°when the maximum strain amplitude was achieved and has strong peaks at 0°and 180°when the minimum strain amplitude was achieved. This indicates that during the cyclic loading, loading direction changes periodically and the orientation of the particle's axes rotated and became periodically horizontal and vertical as a result of cyclic loading. The principal axis of contact normal also deflects periodically along the principal stress axis. Similar results can be found in numerical biaxial test results of saturated gravelly soil under cyclic loading with constant stress amplitude in Wang et al.[21].

Published results have demonstrated that the force-chain evolution is relevant to the mechanical properties of soil [23,24]. Similar concepts can be used to explain the liquefaction behavior of saturated gravelly soil. Fig. 13 shows the force-chain distribution (the distribution of normal contact forces, CForce for short in the figure) varies with axial strains during the cyclic loading process of saturated gravelly soil. The force-chain of the saturated gravelly soil maintains a balanced state at the initial stage. Almost all of the large force-chains are horizontal and vertical. However, under the cyclic loading, the force-chain begins to centralize and several major oblique force-chains forms. The direction of the principal force-chain changes with the direction of the principal stress axis periodically. The maximum magnitude of the principal force-chain also decreases gradually with cyclic loading. The backbone force-chain network is destroyed and magnitude of normal contact force decreases to zero until the initial liquefaction is achieved after several loading-unloading cycles. It can also reveal the meso-mechanical mechanism of liquefaction behavior on saturated gravelly soil. The force-chain distribution can reflect the deflection direction of the principal stress. As also shown in Figs. 12 and 13, the direction of the principal force-chain is consistent with that of the contact normal. Both the fabric and force-chain can reflect the deflection direction of the principal stress.

4. Conclusions

In this study, undrained dynamic triaxial test, CT scan test and numerical simulation are used to explore the liquefaction characteristics of saturated gravelly soil under cyclic loading with constant strain amplitude. The effects of gravel content on liquefaction resistance and meso-mechanism of gravelly soil are analyzed in detail. The major findings from this study and related comments are itemized below:

(1) The liquefaction resistance of gravelly soil may increase considerably with increasing gravel content, which can be explained from the microstructure of gravelly soil obtained by CT can test. For gravel contents between 50% and 80%, it appears that sand particles float in the gravel matrix, and gravel-to-gravel contact became stronger with increasing gravel content.
(2) The numerical simulation results can reflect the macro mechanics phenomenon of saturated gravelly soil liquefaction under cyclic loading with constant strain amplitude, such as pore water pressure accumulation, deviatoric stress amplitude attenuation, initial liquefaction, and state transition in the cyclic triaxial test.
(3) Anisotropy is the most important mechanical properties of gravelly soil liquefaction under cyclic loading with constant strain amplitude. During the cyclic loading, the backbone force-chain network is gradually destroyed and magnitude of normal contact force decreases to zero until the initial liquefaction is achieved after several loading-unloading cycles.
(4) The analysis of fabric and force-chain distribution of saturated gravelly soil during the liquefaction demonstrates a consistent deflection of the principal stress axis. Both of the fabric and force-chain can reflect the deflection direction of the principal stress.

Acknowledgments

This work was financially aided by the National Natural Science Foundations of China (51309027 & 51579237), the Natural Science Foundation of Hubei Province (2015CFB417), the Foundation of State Key Laboratory for Geomechanics and Deep Underground Engineering (SKLGDUEK1110), and the Natural Science Foundation of Zhejiang Province (LY13E080009).

References

[1] Coulter H.W, Migliaccio RR. Effect of the earthquake of March 27, 1964 at Valdez, Alaska, U.S. Geological Survey Professional Paper 542-C; 1966.
[2] Tokimatsu K, Yoshimi Y. Empirical correlation of soil liquefaction based on spt -value and fines content. Soils Found 1983;23(4):56–74.
[3] Wang WS. Earthquake damages to earth dams and levees in relation to soil liquefaction and weakness in soft clays. In: Proceedings of the international conference on case histories in geotechnical engineering, St. Louis, MO. Vol. 1; 1984. 511–21.
[4] Youd TL, Harp EL, Keefer DK, Wilson RC. The Borah Peak, Idaho earthquake of October 28, 1983 – liquefaction. Earthq Spectra, EERI 1985;2(1):71–89.
[5] Yegian MK, Ghahraman VG, Harutiunyan RN. Liquefaction and embankment

failure case histories, 1988 Armenian earthquake. J Geotech Eng 1994;120(3):581–96.
[6] Maurenbrecher PM, Den Outer A, Luger HJ. Review of geotechnical investigations resulting from the Roermond April 13, 1992 earthquake. In: Proceedings of 3rd international conference on recent advances in geotechnical earthquake engineering and soil dynamics, St. Louis, MO; 1995. p. 645–52.
[7] Kokusho T, Tanaka Y, Kudo K., Kawai T. Liquefaction case study of volcanic gravel layer during 1993 Hokkaido-Nansei-Oki earthquake. In: Proceedings of 3rd international conference on recent advances in geotechnical earthquake engineering and soil dynamics, St. Louis, MO; 1995. p. 235–42.
[8] Lin PS, Chang CW. Damage investigation and liquefaction potential analysis of gravelly soil. J Chin Inst Eng 2002;25(5):1–11.
[9] Yuan XM, Cao ZZ, Sun R, et al. Preliminary research on liquefaction characteristic of Wenchuan 8.0 earthquake. Chin J Rock Mech Eng 2009;28(6):1288–96, [in Chinese].
[10] Wong RT, Chan CK, Seed HB. Cyclic loading liquefaction of gravelly soils. J Geotech Eng Div 1975;101(6):571–83.
[11] Baneriee NG., Seed HB, Chan CK. Cyclic behavior of dense coarse-grained materials in relation to dams. No. UCB /EERC(79/13); 1979.
[12] Liu LY, Li G, Bing DP. Earthquake damage of protective layer of white river main dam in Miyun reservoir and vibration liquefaction characteristics of sand gravel material. Beijing: sWater Conservancy Electric Power Press; 1982, [in Chinese].
[13] Wang WS, Chang YP, Zuo XH. Liquefaction characteristics of saturated sand gravel materials under vibration and cyclic loading back and forth. Beijing: Water Conservancy Electric Power Press; 1986, [in Chinese].
[14] Evans MD, Zhou S. Liquefaction behavior of sand-gravel composites. J Geotech Eng 1995;121(3):287–98.
[15] Hatanaka M, Uchida A, Ohara J. liquefaction characteristics of a gravelly fill liquefied during the 1995 Hyogo-Ken Nanbu Earthquake. Soils Found 1997;37(3):107–15.
[16] Kokusho T, Hara T, Hiraoka R. Undrained shear strength of granular soils with different particle gradations. J Geotech Geoenviron Eng 2004;130(6):621–9.
[17] Chang WJ, Chang CW, Zeng JK. Liquefaction characteristics of gap-graded gravelly soils in K0 condition. Soil Dyn Earthq Eng 2014;56:74–85.
[18] Lin PS, Chang CW, Chang WJ. Characterization of liquefaction resistance in gravelly soil: large hammer penetration test and shear wave velocity approach. Soil Dyn Earthq Eng 2004;24(9–10):675–87.
[19] Cao ZZ, Youd TL, Yuan XM. Chinese dynamic penetration test for liquefaction evaluation in gravelly soils. J Geotech Geoenviron Eng 2013;139(8):1320–33.
[20] Hong BN, Liu X. Soil micro-structure theory and experiment. Beijing: Science Press; 2010, [in Chinese].
[21] Wang YL, Cheng ZL, Wang Y, et al. Numerical simulation of liquefaction behavior on gravelly soil in dynamic triaxial test by Particle Flow Code. In: Proceedings of international symposium geomechanics from micro to macro, Cambridge, UK; 2014.
[22] Ibrahim AA, Kagawa T. Microscopic measurement of sand fabric from cyclic tests causing liquefaction. Geotech Test J 1991;14(4):371–82.
[23] Mitchell JK, Soga K. Fundamentals of Soil Behavior, 3rd ed.. New York: Wiley; 2005.
[24] Wang YH, Leung SC. Characterization of cemented sand by experimental and numerical investigations. J Geotech Geoenviron Eng 2008;134(7):992–1004.